

Relativistic corrections in (γ, N) knockout reactions

A. Meucci, C. Giusti, and F. D. Pacati

*Dipartimento di Fisica Nucleare e Teorica, Università di Pavia
and Istituto Nazionale di Fisica Nucleare, Sezione di Pavia, Italy*

November 13, 2018

Abstract

We develop a fully relativistic DWIA model for photonuclear reactions using the relativistic mean field theory for the bound state and the Pauli reduction of the scattering state which is calculated from a relativistic optical potential. Results for the $^{12}\text{C}(\gamma, p)$ and $^{16}\text{O}(\gamma, p)$ differential cross sections and photon asymmetries are displayed in a photon energy range between 60 and 257 MeV, and compared with nonrelativistic DWIA calculations. The effects of the spinor distortion and of the effective momentum approximation for the scattering state are discussed. The sensitivity of the model to different prescriptions for the one-body current operator is investigated. The off-shell ambiguities are large in (γ, p) calculations, and even larger in (γ, n) knockout.

PACS numbers: 25.20.Dc, 24.10.Jv

1 Introduction

The analysis of (γ, N) reactions at photon energies above the giant resonance was the object of a long debate concerning the mechanism of the reaction (see e.g. Ref. [1]). On the one hand, the fact that the experimental cross sections for proton emission can be easily fitted with a single particle wave function addresses to a direct knockout (DKO) mechanism [2]. On the other hand, the transitions with neutron emission, being of the same order of magnitude as those with proton emission, were considered as a clear indication of a quasi-deuteron reaction mechanism [3, 4, 5]. A number of corrections were applied to the DKO model [6, 7] in order to explain both (γ, p) and (γ, n) cross sections, but were unable to give a reasonable explanation of the data.

In recent years, the development of tagged photon facilities allowed to perform experiments with high energy resolution and a clear separation of the different individual states of the residual nucleus. A large number of experimental data was produced at the electron microtron accelerator MAMI-A in Mainz and at the MAX-Laboratory in Lund (see e.g. Refs. [8, 9, 10, 11, 12, 13]).

For the (γ, p) reaction the DKO mechanism represents a large part of the measured cross sections for the low-lying states and in the photon energy range above the giant resonance and below the pion production threshold. The results, however, are very sensitive to the theoretical ingredients adopted for bound and scattering states [2, 14]. Moreover, various calculations in different theoretical approaches indicate that a prominent role is played by more complicated processes, like meson exchange currents (MEC) and multi-step processes due to nuclear correlations [1, 9, 14]. Nonrelativistic calculations based on the distorted wave impulse approximation (DWIA) and with consistent theoretical ingredients

for bound and scattering states (i.e. overlap functions, spectroscopic factors and optical model parameters able to give a good description of $(e, e'p)$ data) are unable to describe (γ, p) data [14, 15, 16]. A reasonable agreement and a consistent description is obtained when the contribution of MEC is added to DKO in the (γ, p) reaction [16]. MEC produce a significant enhancement of the (γ, p) cross sections calculated with DKO and affect both the shape and the magnitude of the angular distributions. For the (γ, n) reaction, where the DKO mechanism gives only a small fraction of the measured cross section, MEC and more complicated processes give the dominant contribution [1, 14, 11].

However, the relative importance of the different mechanisms on (γ, p) and (γ, n) reactions is still not completely understood and justifies the interest on other effects, like relativistic corrections, nuclear current ambiguities and off-shell behavior of the bound nucleons.

The relativistic approach was first applied to (γ, p) reactions in Ref. [17], where also MEC were considered, and in Refs. [18, 19] within the framework of DKO. In these models the wave functions of the bound and continuum nucleons are solutions of a Dirac equation containing appropriate scalar and vector potentials fitted to the ground state properties of the nucleus and to proton-nucleus elastic scattering data. The DKO mechanism was able to reproduce the $^{16}\text{O}(\gamma, p)$ cross section for an incident photon energy of 60 MeV [19]. The same approach was then extended to several target nuclei and to a much wider energy range falling into the Δ -excitation region [20]. The comparison between these calculations and data suggests that DKO is the leading contribution for missing momentum values up to about 500 MeV/ c , while for larger values of the missing momentum an important effect is expected from MEC and Δ -excitation.

Other studies within the same theoretical approach discussed the differences between relativistic and nonrelativistic calculations for (γ, p) and $(e, e'p)$ reactions [21, 22]. They found noticeable medium modifications in the interaction hamiltonian due to relativistic potentials, which suggest that the role of MEC could be strongly modified with respect to a nonrelativistic approach. In any case these relativistic models did not consider the (γ, n) reaction.

Different models based on a fully relativistic DWIA (RDWIA) framework have been developed in recent years and successfully applied to the analysis of $(e, e'p)$ data [23, 24]. In a recent paper [24] we have compared relativistic and nonrelativistic calculations for the $(e, e'p)$ knockout reaction in order to study relativistic effects for cross sections and structure functions and to establish a limit in energy of the validity of a nonrelativistic approach. In this paper we make a similar comparison for (γ, N) reactions. Relativistic effects are different in different situations and kinematics. In (γ, N) at intermediate photon energies the mismatch between the momentum transfer and the momentum of the outgoing nucleon is quite large and larger values of the missing momentum are explored than in usual $(e, e'p)$ experiments. Thus, different effects can be expected for the two reactions. Our aim is to clarify the relationship between the RDWIA and DWIA approaches for (γ, p) and (γ, n) reactions also in comparison with data, and to check the relevance of the DKO mechanism in relativistic and nonrelativistic calculations.

The RDWIA treatment is the same as in Ref. [24]. The relativistic bound state wave functions have been generated as solutions of a Dirac equation containing scalar and vector potentials obtained in the framework of the relativistic mean field theory. The effective Pauli reduction has been adopted for the outgoing nucleon wave function. This scheme appears simpler and is in principle equivalent to the solution of the Dirac equation. The resulting Schrödinger-like equation is solved for each partial wave starting from relativistic optical potentials. In the nonrelativistic calculations, the bound nucleon wave function has

been taken as the normalized upper component of the relativistic four-component spinor and the scattering state is the solution of the same Schrödinger equivalent equation of the relativistic calculation. In order to allow a consistent analysis of $(e, e'p)$ and (γ, p) reactions in comparison with data, RDWIA and DWIA calculations have been performed with the same bound state wave functions and optical potentials used for $(e, e'p)$ in Ref. [24]. The same spectroscopic factors obtained in Ref. [24] by fitting our RDWIA $(e, e'p)$ results to data have been applied to the calculated (γ, N) cross sections.

Results for ^{12}C and ^{16}O target nuclei at different photon energies have been considered for the comparison. The relativistic current is written following the most commonly used current conserving (cc) prescriptions for the $(e, e'p)$ reaction introduced in Ref. [25]. The ambiguities connected with different choices of the electromagnetic current cannot be dismissed. In the $(e, e'p)$ reaction the predictions of different prescriptions are generally in close agreement [26]. Large differences can however be found at high missing momenta [27, 28]. These differences are expected to increase in (γ, N) reactions, where the kinematics is deeply off-shell and higher values of the missing momentum are probed.

The formalism is outlined in Sec. 2. Relativistic and nonrelativistic calculations of the $^{12}\text{C}(\gamma, p)$ and $^{16}\text{O}(\gamma, p)$ cross sections are compared in Sec. 3, where various relativistic effects and current ambiguities are investigated. In Sec. 4 we discuss the role of the DKO mechanism in the description of the (γ, n) reaction. Some conclusions are drawn in Sec. 5.

2 Formalism

The (γ, N) differential cross section can be written as

$$\sigma_\gamma = \frac{2\pi^2\alpha}{E_\gamma} |\mathbf{p}'| E' f_{\text{rec}} f_{11} , \quad (1)$$

where E_γ is the incident photon energy, E' and $|\mathbf{p}'|$ are the energy and the momentum of the emitted nucleon, and f_{rec} is the recoil factor, which is given by

$$f_{\text{rec}}^{-1} = 1 - \frac{E' \mathbf{p}' \cdot \mathbf{p}_{\text{rec}}}{E_{\text{rec}} |\mathbf{p}'|^2} , \quad (2)$$

where E_{rec} and \mathbf{p}_{rec} are the energy and the momentum of the residual recoiling nucleus. In the cross section of Eq. (1) only the transverse response, f_{11} , appears.

If the photon beam is linearly polarized the cross section becomes

$$\sigma_{\gamma,A} = \sigma_\gamma [1 + A \cos(2\phi)] , \quad (3)$$

where ϕ is the angle between the photon polarization and the reaction plane, and A is the photon asymmetry, which can be expressed as the ratio between the interference transverse-transverse and the pure transverse responses

$$A = -\frac{f_{1-1}}{f_{11}} . \quad (4)$$

The structure functions $f_{\lambda\lambda'}$ are defined as bilinear combinations of the nuclear current components, i.e.

$$\begin{aligned} f_{11} &= \langle \mathbf{J}^x (\mathbf{J}^x)^\dagger \rangle + \langle \mathbf{J}^y (\mathbf{J}^y)^\dagger \rangle , \\ f_{1-1} &= \langle \mathbf{J}^y (\mathbf{J}^y)^\dagger \rangle - \langle \mathbf{J}^x (\mathbf{J}^x)^\dagger \rangle , \end{aligned} \quad (5)$$

where $\langle \dots \rangle$ means that average over the initial and sum over the final states is performed fulfilling energy conservation. In our frame of reference the z axis is along \mathbf{q} , and the y axis is parallel to $\mathbf{q} \times \mathbf{p}'$.

In RDWIA the matrix elements of the nuclear current operator, i.e.

$$J^\mu = \int d\mathbf{r} \bar{\Psi}_f(\mathbf{r}) \hat{j}^\mu \exp\{i\mathbf{q} \cdot \mathbf{r}\} \Psi_i(\mathbf{r}), \quad (6)$$

are calculated using relativistic wave functions for initial and final states.

The choice of the electromagnetic operator is, to some extent, arbitrary. Here we discuss the three cc expressions [25, 29, 30]

$$\begin{aligned} \hat{j}_{cc1}^\mu &= G_M(Q^2)\gamma^\mu - \frac{\kappa}{2M}F_2(Q^2)\bar{P}^\mu, \\ \hat{j}_{cc2}^\mu &= F_1(Q^2)\gamma^\mu + i\frac{\kappa}{2M}F_2(Q^2)\sigma^{\mu\nu}q_\nu, \\ \hat{j}_{cc3}^\mu &= F_1(Q^2)\frac{\bar{P}^\mu}{2M} + \frac{i}{2M}G_M(Q^2)\sigma^{\mu\nu}q_\nu, \end{aligned} \quad (7)$$

where $q^\mu = (\mathbf{q}, \omega)$ is the four momentum transfer, $Q^2 = |\mathbf{q}|^2 - \omega^2$, $\bar{P}^\mu = (E + E', \mathbf{p} + \mathbf{p}')$, κ is the anomalous part of the magnetic moment, F_1 and F_2 are the Dirac and Pauli nucleon form factors, $G_M = F_1 + \kappa F_2$ is the Sachs nucleon magnetic form factor, and $\sigma^{\mu\nu} = i/2[\gamma^\mu, \gamma^\nu]$. Since the photon is real, $Q^2 = 0$. In this case F_1 reduces to the nucleon total charge (1 for the proton, and 0 for the neutron), and F_2 to 1. Current conservation is restored by replacing the bound nucleon energy by [25]

$$E = \sqrt{|\mathbf{p}|^2 + M^2} = \sqrt{|\mathbf{p}' - \mathbf{q}|^2 + M^2}. \quad (8)$$

The bound state wave function

$$\Psi_i = \begin{pmatrix} u_i \\ v_i \end{pmatrix}, \quad (9)$$

is given by the Dirac-Hartree solution of a relativistic Lagrangian containing scalar and vector potentials.

The ejectile wave function Ψ_f is written in terms of its positive energy component Ψ_{f+} following the direct Pauli reduction method

$$\Psi_f = \begin{pmatrix} \Psi_{f+} \\ \frac{\boldsymbol{\sigma} \cdot \mathbf{p}'}{M + E' + S - V} \Psi_{f+} \end{pmatrix}, \quad (10)$$

where $S = S(r)$ and $V = V(r)$ are the scalar and vector potentials for the nucleon with energy E' . The upper component Ψ_{f+} can be related to a Schrödinger equivalent wave function Φ_f by the Darwin factor $D(r)$, i.e.

$$\Psi_{f+} = \sqrt{D(r)}\Phi_f, \quad (11)$$

$$D(r) = \frac{M + E' + S - V}{M + E'}. \quad (12)$$

Φ_f is a two-component wave function which is solution of a Schrödinger equation containing equivalent central and spin-orbit potentials obtained from the scalar and vector

potentials [22]. Hence, using the relativistic normalization, the emitted nucleon wave function is written as

$$\begin{aligned}\bar{\Psi}_f &= \Psi_f^\dagger \gamma^0 = \sqrt{\frac{M+E'}{2E'}} \left[\left(\frac{1}{\sigma \cdot \mathbf{p}'} \right) \sqrt{D} \Phi_f \right]^\dagger \gamma^0 \\ &= \sqrt{\frac{M+E'}{2E'}} \Phi_f^\dagger (\sqrt{D})^\dagger \left(1 ; \sigma \cdot \mathbf{p}' \frac{1}{C^\dagger} \right) \gamma^0 ,\end{aligned}\quad (13)$$

where

$$C = C(r) = M + E' + S(r) - V(r) . \quad (14)$$

If we substitute Eqs. (9) and (13) into Eq. (6) and choose one of the current conserving prescriptions of Eq. (7), we obtain the relativistic expressions of the nuclear current

$$\begin{aligned}\mathbf{J}_{cc1} &= \sqrt{\frac{E'+M}{2E'}} \int d\mathbf{r} \Phi_f^\dagger (\sqrt{D})^\dagger \left\{ G_M \left[\sigma v_i - i(\sigma \cdot \nabla) \frac{1}{C^\dagger} \sigma u_i \right] \right. \\ &\quad \left. + \frac{\kappa}{2M} F_2 \left[(2i\nabla + \mathbf{q}) u_i + i(\sigma \cdot \nabla) \frac{1}{C^\dagger} (2i\nabla + \mathbf{q}) v_i \right] \right\} \exp\{i\mathbf{q} \cdot \mathbf{r}\} ,\end{aligned}\quad (15)$$

$$\begin{aligned}\mathbf{J}_{cc2} &= \sqrt{\frac{E'+M}{2E'}} \int d\mathbf{r} \Phi_f^\dagger (\sqrt{D})^\dagger \left\{ F_1 \left[-i(\sigma \cdot \nabla) \frac{1}{C^\dagger} \sigma u_i + \sigma v_i \right] \right. \\ &\quad \left. + i \frac{\kappa}{2M} F_2 \left[\sigma \times \mathbf{q} u_i + \omega(\sigma \cdot \nabla) \frac{1}{C^\dagger} \sigma u_i \right. \right. \\ &\quad \left. \left. - i\omega \sigma v_i + i(\sigma \cdot \nabla) \frac{1}{C^\dagger} \sigma \times \mathbf{q} v_i \right] \right\} \exp\{i\mathbf{q} \cdot \mathbf{r}\} ,\end{aligned}\quad (16)$$

$$\begin{aligned}\mathbf{J}_{cc3} &= \sqrt{\frac{E'+M}{2E'}} \int d\mathbf{r} \Phi_f^\dagger (\sqrt{D})^\dagger \\ &\quad \left\{ \frac{i}{2M} F_1 \left[(-2i\nabla - \mathbf{q}) u_i - i(\sigma \cdot \nabla) \frac{1}{C^\dagger} (2i\nabla + \mathbf{q}) v_i \right] \right. \\ &\quad \left. + \frac{i}{2M} G_M \left[\sigma \times \mathbf{q} u_i + \omega(\sigma \cdot \nabla) \frac{1}{C^\dagger} \sigma u_i \right. \right. \\ &\quad \left. \left. - i\omega \sigma v_i + i(\sigma \cdot \nabla) \frac{1}{C^\dagger} \sigma \times \mathbf{q} v_i \right] \right\} \exp\{i\mathbf{q} \cdot \mathbf{r}\} ,\end{aligned}\quad (17)$$

where the \bar{P} operator has been replaced by the gradient $-2i\nabla - \mathbf{q}$, which operates not only on the components of the Dirac spinor but also on $\exp\{i\mathbf{q} \cdot \mathbf{r}\}$. It is interesting to notice that in Eqs. (15) and (17) appear terms which are proportional to the second derivative of the lower component of the Dirac spinor.

3 The (γ, p) reaction

The (γ, p) reaction is an interesting process for testing our RDWIA program and investigating the differences with respect to the DWIA approach. At intermediate photon energies there is a large difference between the incoming photon and outgoing nucleon momenta and missing momentum values higher than in usual $(e, e'p)$ experiments are explored. Thus, different relativistic effects can be expected in the two reactions. Moreover, it can be interesting to check the relevance of the DKO mechanism in comparison with data for corresponding RDWIA and DWIA calculations with consistent theoretical ingredients for

bound and scattering states. Previous RDWIA analyses [20] suggest that DKO is the leading contribution to the (γ, p) cross section for low values of E_γ and not too large values of the missing momentum. In contrast, in nonrelativistic calculations the DKO mechanism generally underestimates the experimental cross sections and an important contribution is given by MEC even at low photon energies. In these investigations, however, RDWIA and DWIA calculations make generally use of different bound state wave functions and optical potentials, and (γ, p) results are very sensitive to the theoretical ingredients adopted in the calculations.

A large amount of experiments were carried out in the past on several target nuclei and over a wide range of photon energies. Here, we have performed calculations for ^{12}C and ^{16}O . The bound state wave functions and optical potentials are the same as in the analysis of Ref. [24], where the RDWIA results are in satisfactory agreement with $(e, e'p)$ data. In order to allow a consistent comparison with data, the same spectroscopic factors obtained by fitting our RDWIA $(e, e'p)$ calculations [24] to data have been here applied to the (γ, p) results, that is 0.56 for ^{12}C and 0.70 for ^{16}O .

The relativistic bound state wave function has been generated using the program ADFX of Ref. [31], where relativistic Hartree-Bogoliubov equations are solved. The model starts from a Lagrangian density containing sigma-, omega-, rho-meson, and photon fields, whose potentials are obtained by solving self-consistently Klein-Gordon equations.

The corresponding wave function for the nonrelativistic calculation has been taken as the upper component of the relativistic four-component spinor, which is normalized to 1 in coordinate and spin space. Presumably, this is not the best choice for the nonrelativistic DWIA calculations, but the same ingredients are to be used in order to perform a clear comparison between the two approaches.

The outgoing nucleon wave function is calculated by means of the complex phenomenological optical potential of Ref. [32], obtained from fits to proton elastic scattering data in an energy range up to 1040 MeV. The Schrödinger equivalent potentials calculated in the same way were used in the nonrelativistic program.

Since no rigorous prescription exists for handling off-shell nucleons, it is worthwhile to study the sensitivity of one nucleon photoemission to different choices of the nuclear current.

The nonrelativistic current is written as an expansion up to order $1/M^2$ from a Foldy-Wouthuysen transformation [33, 34] applied to the interaction Hamiltonian where the nuclear current is in the $cc2$ form of Eq. (7). Thus, the $cc2$ prescription for the relativistic nuclear current is more appropriate in the comparison between the relativistic and nonrelativistic models.

3.1 Relativistic and nonrelativistic calculations

In this section the results of the comparison between our RDWIA and DWIA calculations are discussed. One has to remember that our nonrelativistic code contains some relativistic corrections in the kinematics and in the nuclear current through the expansion in $1/M$. This means that the nonrelativistic results cannot be obtained from the relativistic program simply by neglecting the lower components of the Dirac spinor and applying the proper normalization.

The comparison between the RDWIA and DWIA results is shown in Fig. 1 for the cross section of the $^{16}\text{O}(\gamma, p)^{15}\text{N}_{\text{g.s.}}$ reaction. The photon energy range is taken between 60 MeV and 257 MeV, but the nonrelativistic calculations are not extended above 200 MeV [24]. In the considered energy range missing momentum values between about 200 and 1000

MeV/ c are explored.

We see that the differences between the nonrelativistic calculations and the relativistic ones with the $cc2$ prescription are sensible at all energies. The nonrelativistic results are always smaller than the data [9, 35, 36, 37]. This effect was already known from previous nonrelativistic analyses and suggested that MEC must give an important contribution to the cross section. On the contrary, the relativistic results are generally closer to the data and well reproduce the magnitude and shape, at least at low energies. This result is in agreement with similar RDWIA approaches with the $cc2$ current [18, 19, 20]. For higher energies, the relativistic results fall below the data and the discrepancies increase with the proton angle. This seems to indicate that the DKO mechanism gives the most important contribution to the cross section at lower missing momenta, while more complicated processes such as MEC and Δ -excitations become more and more important at larger missing momenta.

In Fig. 2 the photon asymmetries are shown in the same kinematics as in Fig. 1. The differences between DWIA and RDWIA results with $cc2$ are small at 60 MeV, but rapidly increase with the photon energy.

In Fig. 3 the cross section for the $^{12}\text{C}(\gamma, p)^{11}\text{B}_{\text{g.s.}}$ reaction is presented. The nonrelativistic results are also in this case smaller than the relativistic ones, but the most apparent feature is that both results lie above the data [8, 38]. The fact that RDWIA calculations with the $cc2$ current overestimate the data by a factor of 2 was already pointed out in Ref. [20]. A better description of data might be obtained with a more careful determination of the ^{12}C ground state which should include its intrinsic deformation.

3.2 Current ambiguities

In this section the sensitivity of (γ, p) calculations to different choices of the nuclear current is discussed. In the case of one proton knockout the expressions for the electromagnetic nuclear current of Eq. (7) reduce to

$$\begin{aligned}\hat{j}_{cc1}^{\mu} &= \gamma^{\mu} + \kappa_p \left(\gamma^{\mu} - \frac{\bar{P}^{\mu}}{2M} \right), \\ \hat{j}_{cc2}^{\mu} &= \gamma^{\mu} + i \frac{\kappa_p}{2M} \sigma^{\mu\nu} q_{\nu}, \\ \hat{j}_{cc3}^{\mu} &= \frac{\bar{P}^{\mu}}{2M} + \frac{i}{2M} (1 + \kappa_p) \sigma^{\mu\nu} q_{\nu},\end{aligned}\tag{18}$$

where $\kappa_p = 1.793$ is the anomalous part of the proton magnetic moment. These expressions are obviously equivalent for a free nucleon, but give different results for an off-shell nucleon.

It is interesting to notice that the nonrelativistic reductions of the three cc forms give identical results up to order $1/M$ following the direct Pauli reduction scheme in the limit of no Dirac S and V potentials and $M + E = 2M$. The equivalence of Pauli reduction and Foldy-Wouthuysen transformation up to order $1/M$ was already pointed out in Refs. [39, 22].

The results obtained with different current operators are displayed and compared for ^{16}O in Fig. 1. The differences are large. We have already noticed that the $cc2$ results are in satisfactory agreement with the experimental data at lower energies, but they tend to fall down with increasing proton angle and photon energy. RDWIA results are strongly enhanced if we use $cc1$ current. This is probably due to a too small interference term which does not correctly estimate the convective current contained in both γ^{μ} and $\bar{P}^{\mu}/(2M)$ terms when the nucleon is off-shell. Also in Ref. [27], in an $(e, e'p)$ analysis within the

framework of the relativistic plane wave impulse approximation, large differences are found between results obtained with the *cc2* and *cc1* prescriptions for high values of the missing momentum and significantly higher cross sections are obtained with *cc1*. The results with the *cc3* current in Fig. 1 are more similar to the *cc2* ones. At low energy *cc3* lies below *cc2*, but the differences rapidly decrease with the energy.

In Fig. 2 a comparison of photon asymmetry calculations in the same kinematics as in Fig. 1 is shown. The differences are sensible already at 60 MeV and tend to increase with the energy.

Large ambiguities are found also in the case of $^{12}\text{C}(\gamma, p)$ reaction (Fig. 3). Results obtained with the *cc1* current are enhanced above the data by an order of magnitude. On the contrary, *cc3* results are smaller than the data.

3.3 Spinor distortion and Darwin factor

The optical potential enters into the Darwin factor D , which multiplies the Schrödinger equivalent eigenfunction, and into the spinor distortion C , which is applied only to the lower component of Dirac spinor. The distortion of the scattering wave function is calculated through a partial wave expansion and it is always included in the calculations. The Darwin factor gives a reduction of the cross section. On the contrary, the spinor distortion produces an enhancement.

The combined effects of the two corrections are displayed and compared in Figs. 4 and 5 for the cross section of the reaction $^{16}\text{O}(\gamma, p)^{15}\text{N}_{\text{g.s.}}$ at $E_\gamma = 60$ and 196 MeV. Results without the Darwin factor and spinor distortion at 60 MeV using either *cc1* or *cc2* are reduced with respect to the full calculations, while results with *cc3* are enhanced for low scattering angles. These effects decrease at 196 MeV, where calculations without potentials are closer to full calculations.

3.4 Effective momentum approximation

The EMA prescription, which consists in evaluating the momentum operator in the nuclear current using the asymptotic value of the ejected nucleon momentum, strongly simplifies the calculations. This approximation was successfully used in some $(e, e'p)$ calculations, and, in particular, in the model of Refs. [29, 30] for bound and scattering states. Since in our approach the bound state wave function is solution of a Dirac equation, we investigate the EMA effects only for the scattering states. We have to notice that in the nuclear current the EMA prescription affects only the \bar{P}^μ term in *cc1* and *cc3* formulae, while *cc2* is unchanged. However, a momentum dependence comes from the Pauli reduction of the scattering wave function.

The effects of EMA are displayed and compared with the full RDWIA results in Figs. 4 and 5 at $E_\gamma = 60$ and 196 MeV. At 60 MeV the differences are large, but they decrease with the energy and become much smaller at 196 MeV. This behavior is practically independent of the nuclear current. This can be understood if we consider that distortion effects decrease with the energy, so that at high energy DWIA results are more similar to PWIA ones, where EMA is exact.

4 The (γ, n) reaction

In this section relativistic effects are discussed for the (γ, n) reaction. The experimental angular distributions are similar in magnitude and shape to those obtained for the (γ, p)

reaction. The ratio between the (γ, p) and (γ, n) cross sections is comparable to unity and suggests a two-body mechanism. In fact, nonrelativistic calculations based on the DKO mechanism give but a small fraction of the measured cross sections.

In order to test the relevance of the DKO contribution, we have performed RDWIA and DWIA calculations for the $^{16}\text{O}(\gamma, n)^{15}\text{O}_{\text{g.s.}}$ reaction. For neutron knockout the electromagnetic nuclear current of Eq. (7) reduces to the anomalous spin current only, i.e.

$$\begin{aligned}\hat{j}_{cc1}^{\mu} &= \kappa_n \left(\gamma^{\mu} - \frac{\bar{P}^{\mu}}{2M} \right) , \\ \hat{j}_{cc2}^{\mu} &= \hat{j}_{cc3}^{\mu} = i \frac{\kappa_n}{2M} \sigma^{\mu\nu} q_{\nu} ,\end{aligned}\tag{19}$$

where $\kappa_n = -1.913$ is the anomalous part of the neutron magnetic moment. Notice that $\hat{j}_{cc2}^{\mu} = \hat{j}_{cc3}^{\mu}$, while for *cc1* the spin current is written by means of a difference between the Dirac current γ^{μ} and the convective current $\bar{P}^{\mu}/(2M)$.

In Fig. 6 relativistic and nonrelativistic results for the $^{16}\text{O}(\gamma, n)^{15}\text{O}_{\text{g.s.}}$ reaction are shown in comparison with data [11, 40, 41]. The same spectroscopic factor as in the corresponding (γ, p) reaction has been applied to the calculated results.

We see that neither nonrelativistic nor relativistic *cc2* (*cc3*) calculations reproduce the magnitude of experimental data. This result is not surprising. It confirms what was already found in previous DWIA calculations and indicates that more complicated two-body effects are needed to reproduce the data. Relativistic results are strongly enhanced if we use the *cc1* current. This effect is particularly surprising at $E_{\gamma} = 150$ and 200 MeV, where the *cc1* curve fits the data. This result can be attributed to the $\gamma^{\mu} - \bar{P}^{\mu}/(2M)$ operator, which does not correctly describe the spin current when the kinematics is deeply off-shell, and, therefore, is to be considered unreliable.

The differences between the DWIA and RDWIA results with *cc2* are large. They are reduced if we perform nonrelativistic calculations with a nuclear current expanded up to order $1/M^3$ [34], but the contribution of the third order is very large for this reaction, and comparable to the second order one.

5 Summary and conclusions

In this paper we have presented relativistic and nonrelativistic DWIA calculations for (γ, N) reactions on ^{12}C and ^{16}O , in a photon-energy range between 60 and 257 MeV, in order to check the relevance of the DKO mechanism in RDWIA and DWIA models and investigate relativistic effects.

The transition matrix element of the nuclear current operator is calculated in RDWIA using the bound state wave functions obtained in the framework of the relativistic mean field theory, and the direct Pauli reduction method with scalar and vector potentials for the ejectile wave functions. In order to study the ambiguities in the electromagnetic vertex due to the off-shellness of the initial nucleon, we have performed calculations using three current conserving expressions. The nonrelativistic DWIA matrix elements are computed in a similar way to allow a direct comparison with the relativistic results. In order to allow a consistent comparison of $(e, e'p)$ and (γ, p) data, calculations have been performed with the same bound state wave functions, spectroscopic factors and optical potentials as in our recent $(e, e'p)$ analysis of Ref. [24].

Nonrelativistic (γ, p) results are always smaller than the data and suggest the idea that MEC are relevant even at low energies. On the contrary, RDWIA calculations seem to

indicate that the DKO mechanism is the leading process, at least for low photon energies. These results are in substantial agreement with previous DWIA and RDWIA analyses.

We have discussed the sensitivity of the (γ, p) reaction to the different choices of the nuclear current. Unlike the case of the $(e, e'p)$ reaction, large ambiguities are generally found. Results with the *cc2* current are in satisfactory agreement with the experimental data at lower energies, but they tend to fall down with increasing proton angle and photon energy. On the contrary, the results with *cc1* are strongly enhanced. This result seems due to a too small interference term which overestimates the convective current when the initial nucleon is off-shell. The results with *cc3* are more similar to the *cc2* ones. The differences decrease when the energy increases.

The effect of the scalar and vector potentials in the Pauli reduction for the scattering state has been discussed. These potentials appear in the relativistic treatment and are absent in the nonrelativistic one. The combined contribution of the Darwin factor, which reduces the cross section, and of the spinor distortion, which enhances the effects of the lower components of the Dirac spinor, is important at low E_γ , and decreases at higher energies.

The validity of EMA in the scattering state of relativistic calculations has been investigated. The differences with respect to the exact result are large at low photon energies, but rapidly decrease and become small at higher energies.

Relativistic calculations of the (γ, n) cross sections give huge off-shell ambiguities. The *cc2* and *cc3* prescriptions coincide in the neutron case, but the enhancement obtained with *cc1* is dramatic and brings the RDWIA results above the data at $E_\gamma = 60$ MeV and in good agreement with data at $E_\gamma = 150$ and 200 MeV. However, we cannot argue that the DKO mechanism with the *cc1* prescription correctly describes (γ, n) cross sections. This result is due to a dominant off-shell effect on the *cc1* current operator, which does not correctly describe the modest contribution from the spin current.

Neither nonrelativistic DWIA nor RDWIA calculations with *cc2* reproduce (γ, n) data. There are sensible differences between the results of the two approaches, but in both cases the experimental cross sections are largely underestimated. This is an indication of the dominance of two-body mechanisms in the (γ, n) reaction. A careful and consistent evaluation of these mechanisms within relativistic and nonrelativistic frameworks for (γ, n) and (γ, p) reactions would be highly desirable and helpful to draw conclusions about the reaction mechanism and to solve the present ambiguities.

References

- [1] S. Boffi, C. Giusti, F. D. Pacati, and M. Radici, *Electromagnetic Response of Atomic Nuclei*, Oxford Studies in Nuclear Physics (Clarendon Press, Oxford, 1996).
- [2] S. Boffi, C. Giusti, and F. D. Pacati, Nucl. Phys. **A358**, 91 (1981).
- [3] J. S. Levinger, Phys. Rev. **84**, 43 (1951); Phys. Lett. **B82**, 181 (1979).
- [4] B. Schoch, Phys. Rev. Lett. **41**, 80 (1970).
- [5] J. A. Eden *et al.*, Phys. Rev. C **44**, 753 (1991).
- [6] S. Boffi, R. Cenni, C. Giusti, and F. D. Pacati, Nucl. Phys. **A420**, 38 (1984).
- [7] S. Boffi, F. Capuzzi, C. Giusti, and F. D. Pacati, Nucl. Phys. **A436**, 438 (1985).
- [8] S. V. Springham *et al.*, Nucl. Phys. **A517**, 93 (1990).

- [9] G. J. Miller *et al.*, Nucl. Phys. **A586**, 125 (1995).
- [10] C. Van den Abeele, D. Ryckbosch, J. Dias, L. Van Hoorebeke, R. Van de Vyver, J. O. Adler, K. Hansen, L. Isaksson, H. Ruijter, and B. Schröder, Nucl. Phys. **A586**, 281 (1995).
- [11] B. E. Andersson *et al.*, Phys. Rev. C **51**, 2553 (1995).
- [12] L. J. de Bever *et al.*, Phys. Rev. C **58**, 981 (1998).
- [13] D. Branford *et al.*, Phys. Rev. C **63**, 014310 (2001).
- [14] G. Benenti, C. Giusti, and F. D. Pacati, Nucl. Phys. **A574**, 716 (1994).
- [15] D. G. Ireland and G. van der Steenhoven, Phys. Rev. C **49**, 2182 (1994).
- [16] M. K. Gaidarov, K. A. Pavlova, A. N. Antonov, M. V. Stoitsov, S. S. Dimitrova, M. V. Ivanov, and C. Giusti, Phys. Rev. C **61**, 014306 (2000);
M. V. Ivanov, M. K. Gaidarov, A. N. Antonov, and C. Giusti, Phys. Rev. C **64**, 014605 (2001).
- [17] J. P. McDermott, E. Rost, J. R. Shepard, and C. Y. Cheung, Phys. Rev. Lett. **61**, 814 (1988).
- [18] G. M. Lotz and H. S. Sherif, Nucl. Phys. **A537**, 285 (1992).
- [19] J. I. Johansson, H. S. Sherif, and G. M. Lotz, Nucl. Phys. **A605**, 517 (1996).
- [20] J. I. Johansson and H. S. Sherif, Phys. Rev. C **56**, 328 (1997).
- [21] M. Hedayati-Poor and H. S. Sherif, Phys. Lett. **B326**, 9 (1994).
- [22] M. Hedayati-Poor, J. I. Johansson, and H. S. Sherif, Nucl. Phys. **A593**, 377 (1995).
- [23] Y. Jin, D. S. Onley, and L. E. Wright, Phys. Rev. C **45**, 1311 (1992);
Y. Jin and D. S. Onley, Phys. Rev. C **50**, 377 (1994);
J. M. Udías, P. Sarriguren, E. Moya de Guerra, E. Garrido, and J. A. Caballero, Phys. Rev. C **48**, 2731 (1993);
J. M. Udías, P. Sarriguren, E. Moya de Guerra, E. Garrido, and J. A. Caballero, Phys. Rev. C **51**, 3246 (1995);
J. M. Udías, P. Sarriguren, E. Moya de Guerra, and J. A. Caballero, Phys. Rev. C **53**, R1488 (1996);
J. M. Udías and J. R. Vignote Phys. Rev. C **62**, 034302 (2000).
- [24] A. Meucci, C. Giusti, and F. D. Pacati, Phys. Rev. C **64**, 014604 (2001).
- [25] T. de Forest, Jr., Nucl. Phys. **A392**, 232 (1983).
- [26] S. Pollock, H. W. L. Naus, and J. H. Koch, Phys. Rev. C **53**, 2304 (1996).
- [27] J. A. Caballero, T. W. Donnelly, E. Moya de Guerra, J. M. Udías, Nucl. Phys. **A632**, 323 (1998).
- [28] S. Jeschonnek and J. W. Van Orden, Phys. Rev. C **62**, 044613 (2000).
- [29] J. J. Kelly, Phys. Rev. C **56**, 2672 (1997); **59**, 3256 (1999).

- [30] J. J. Kelly, Phys. Rev. C **60**, 044609 (1999).
- [31] W. Pöschl, D. Vretenar, and P. Ring, Comput. Phys. Commun. **103**, 217 (1997).
- [32] E. D. Cooper, S. Hama, B. C. Clark, and R. L. Mercer, Phys. Rev. C **47**, 297 (1993).
- [33] L. L. Foldy and S. A. Wouthuysen, Phys. Rev. **78**, 29 (1950).
- [34] C. Giusti and F. D. Pacati, Nucl. Phys. **A336**, 427 (1980).
- [35] D. J. S. Findlay and R. O. Owens, Nucl. Phys. **A279**, 385 (1977).
- [36] M. J. Leitch, J. L. Matthews, W. W. Sapp, C. P. Sargent, S. A. Wood, D. J. S. Findlay, R. O. Owens, and B. L. Roberts, Phys. Rev. C **31**, 1633 (1985).
- [37] G. S. Adams, E. R. Kinney, J. L. Matthews, W. W. Sapp, T. Soos, R. O. Owens, R. S. Turley, and G. Pignault, Phys. Rev. C **38**, 2771 (1988).
- [38] A. C. Shotter, S. Springham, D. Branford, J. Yorkston, J. C. McGeorge, B. Schoch, and P. Jennewein, Phys. Rev. C **37**, 1354 (1988).
- [39] H. W. Fearing, G. I. Poulis, and S. Scherer, Nucl. Phys. **A570**, 657 (1994).
- [40] H. Goringe, B. Schoch, and G. Lührs, Nucl. Phys. **A384**, 414 (1982).
- [41] E. J. Beise *et al.*, Phys. Rev. Lett. **62**, 2593 (1989).

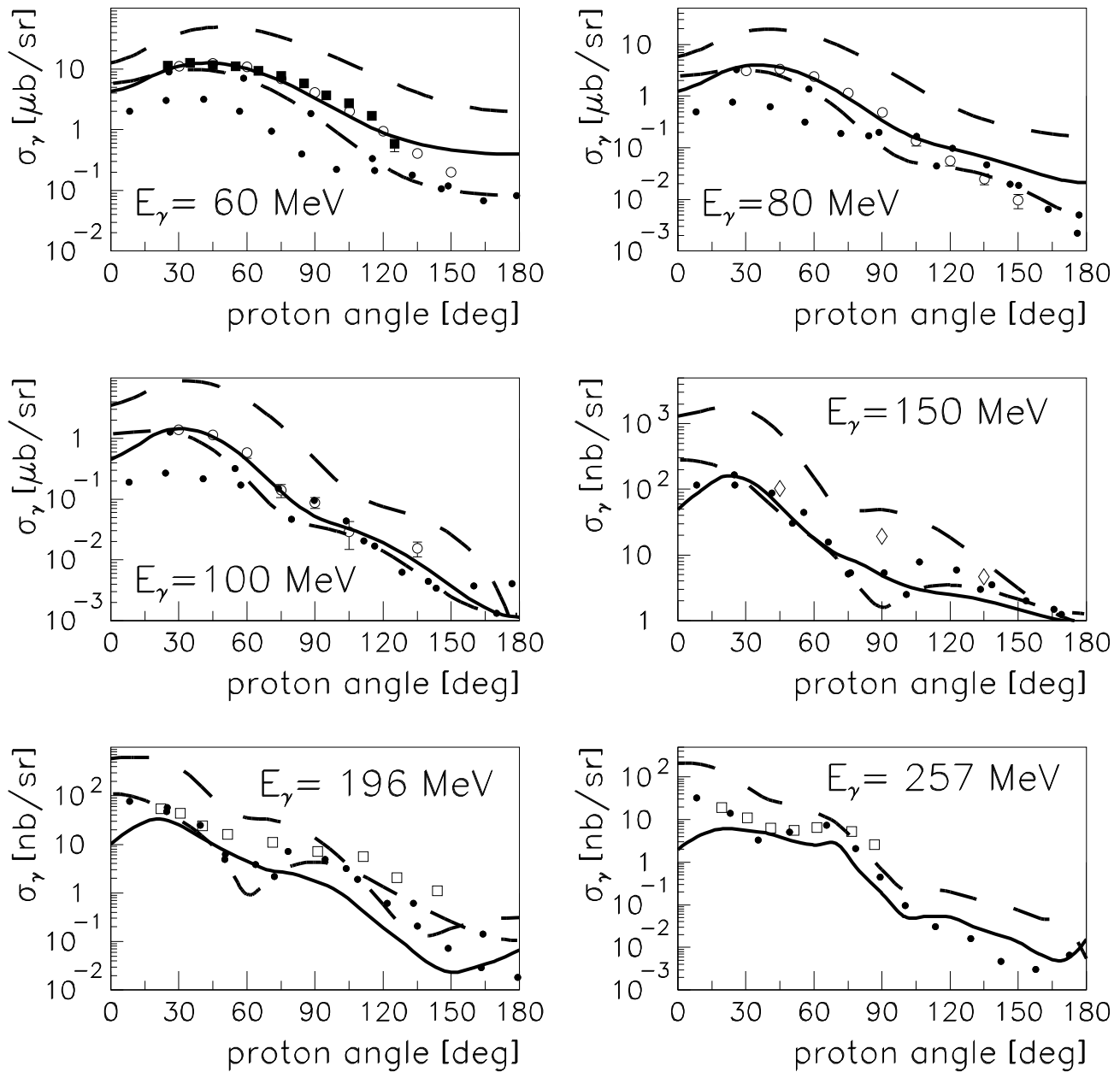


Figure 1: The cross section for the $^{16}\text{O}(\gamma, p)^{15}\text{N}_{\text{g.s.}}$ reaction as a function of the proton scattering angle for photon energies ranging from 60 to 257 MeV. The data at 60 MeV are from Ref. [9] (black squares) and from Ref. [35] (open circles). The data at 80 and 100 MeV are from Ref. [35]. The data at 150 MeV are from Ref. [36], and those at 196 and 257 MeV are from Ref. [37]. Results shown correspond to RDWIA calculations with the *cc2* (solid line), *cc1* (dashed line), and *cc3* (dotted line) current. The dot-dashed line is the nonrelativistic result.

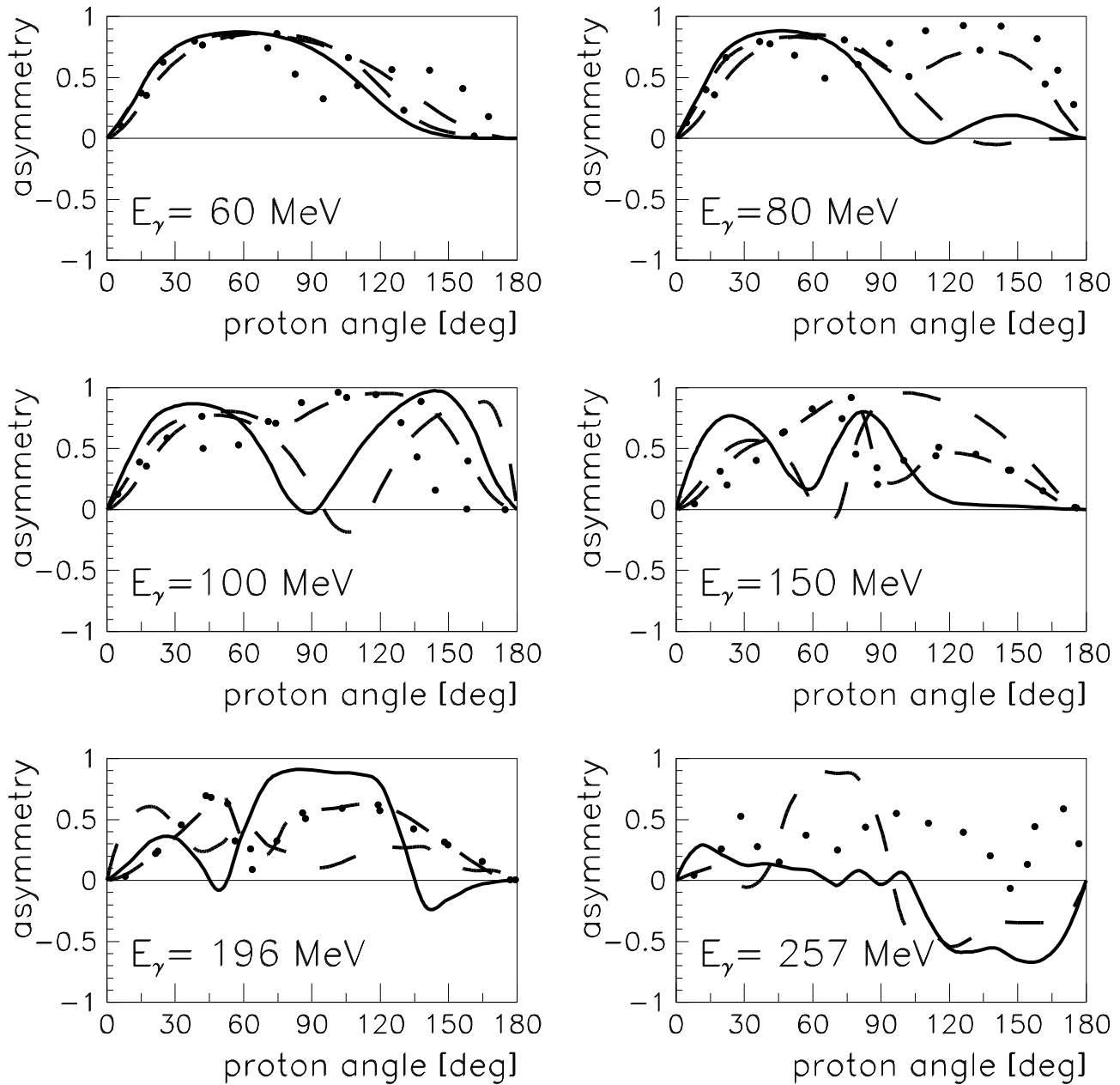


Figure 2: The same as in Fig. 1, but for the photon asymmetry.

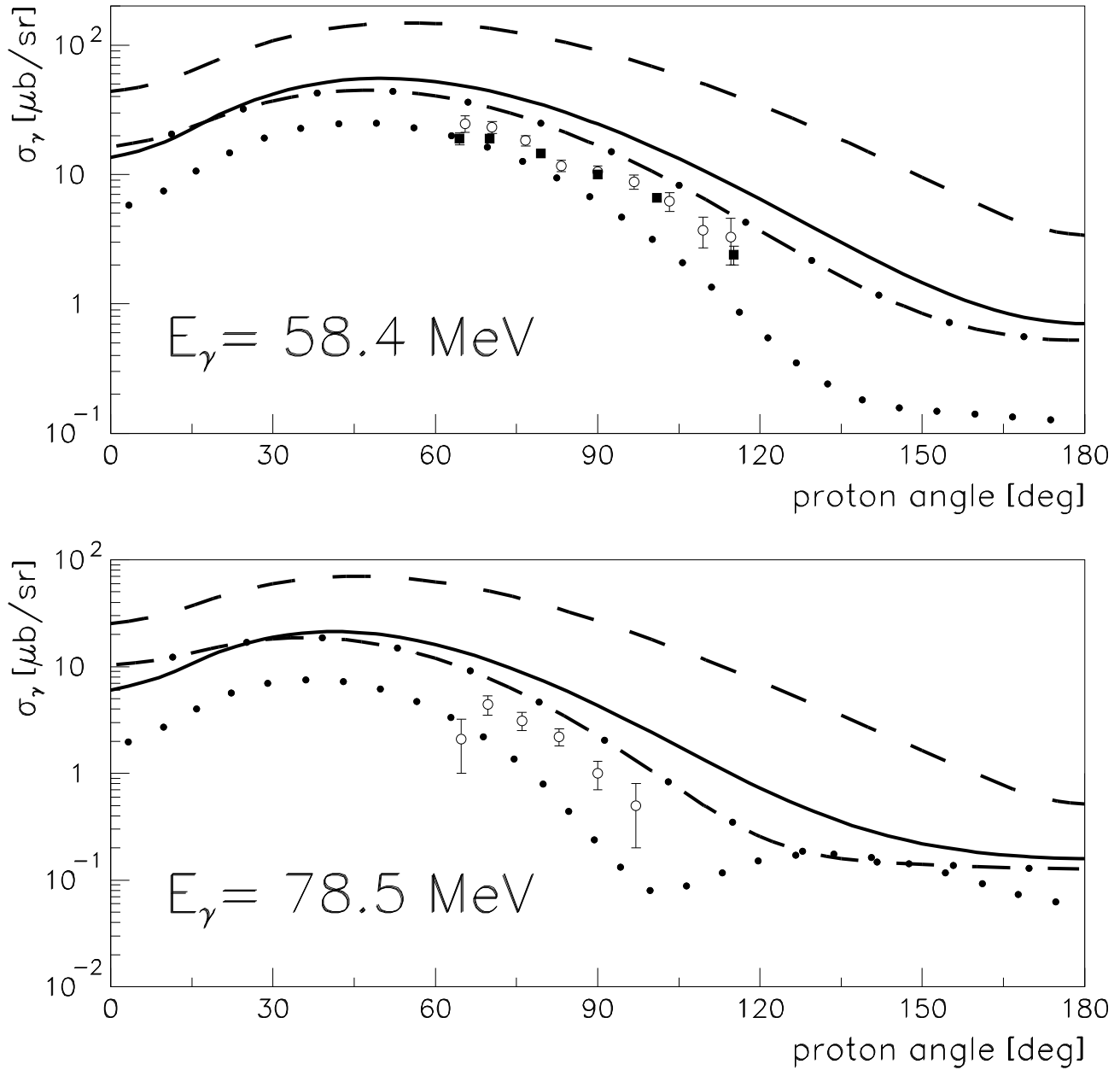


Figure 3: The cross section for the $^{12}\text{C}(\gamma, p)^{11}\text{B}_{\text{g.s.}}$ reaction as a function of the proton scattering angle at $E_\gamma = 58.4$ and 78.5 MeV. The data are from Ref. [38] (black squares) and from Ref. [8] (open circles). Line convention as in Fig. 1.

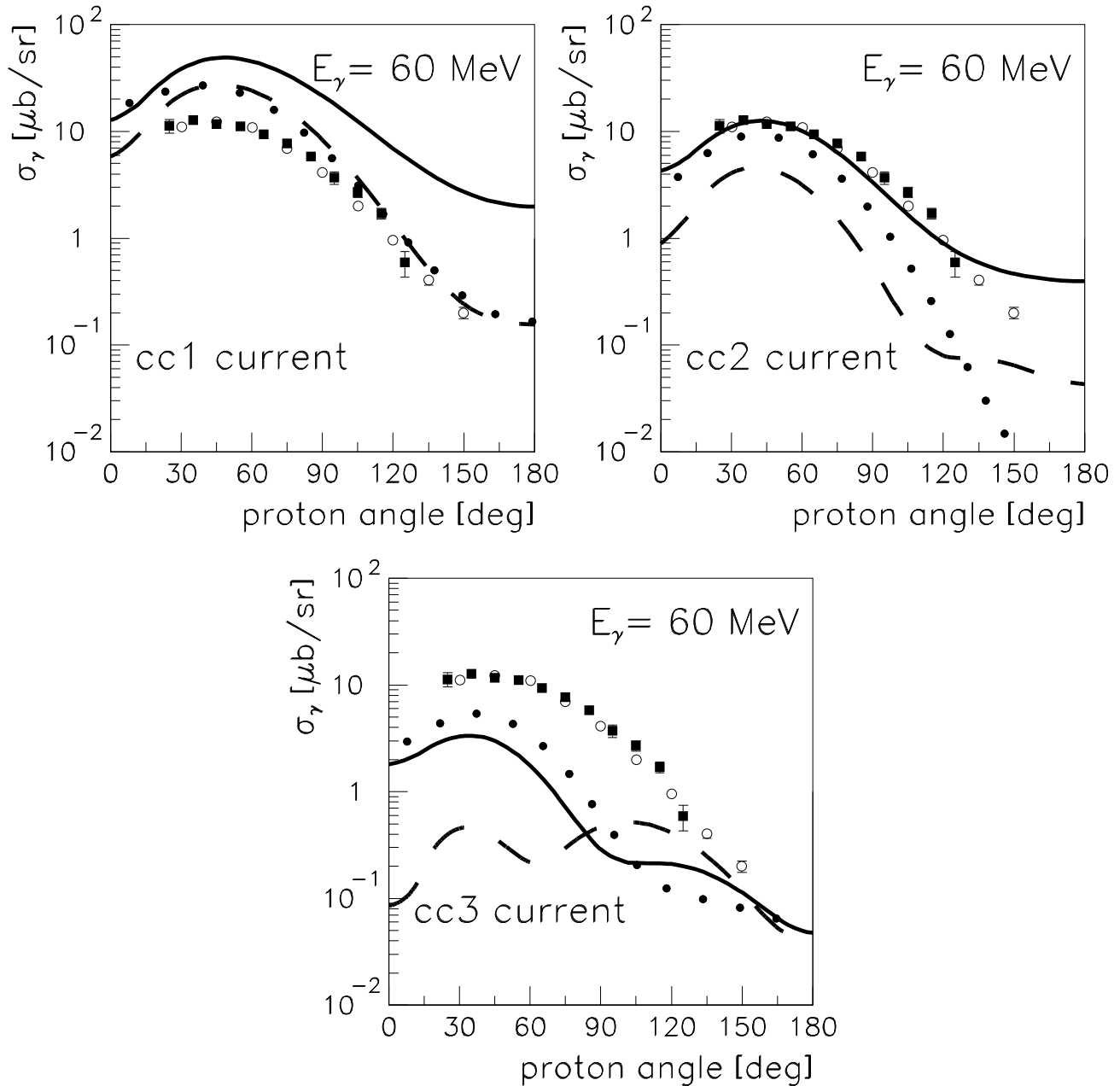


Figure 4: The cross section for the $^{16}\text{O}(\gamma, p)^{15}\text{N}_{\text{g.s.}}$ reaction as a function of the proton scattering angle at $E_\gamma = 60$ MeV. The data are from Ref. [9] (black squares) and from Ref. [35] (open circles). The solid lines give the RDWIA results, the dotted lines the calculations without the Darwin factor and spinor distortion, and the dashed lines the EMA.

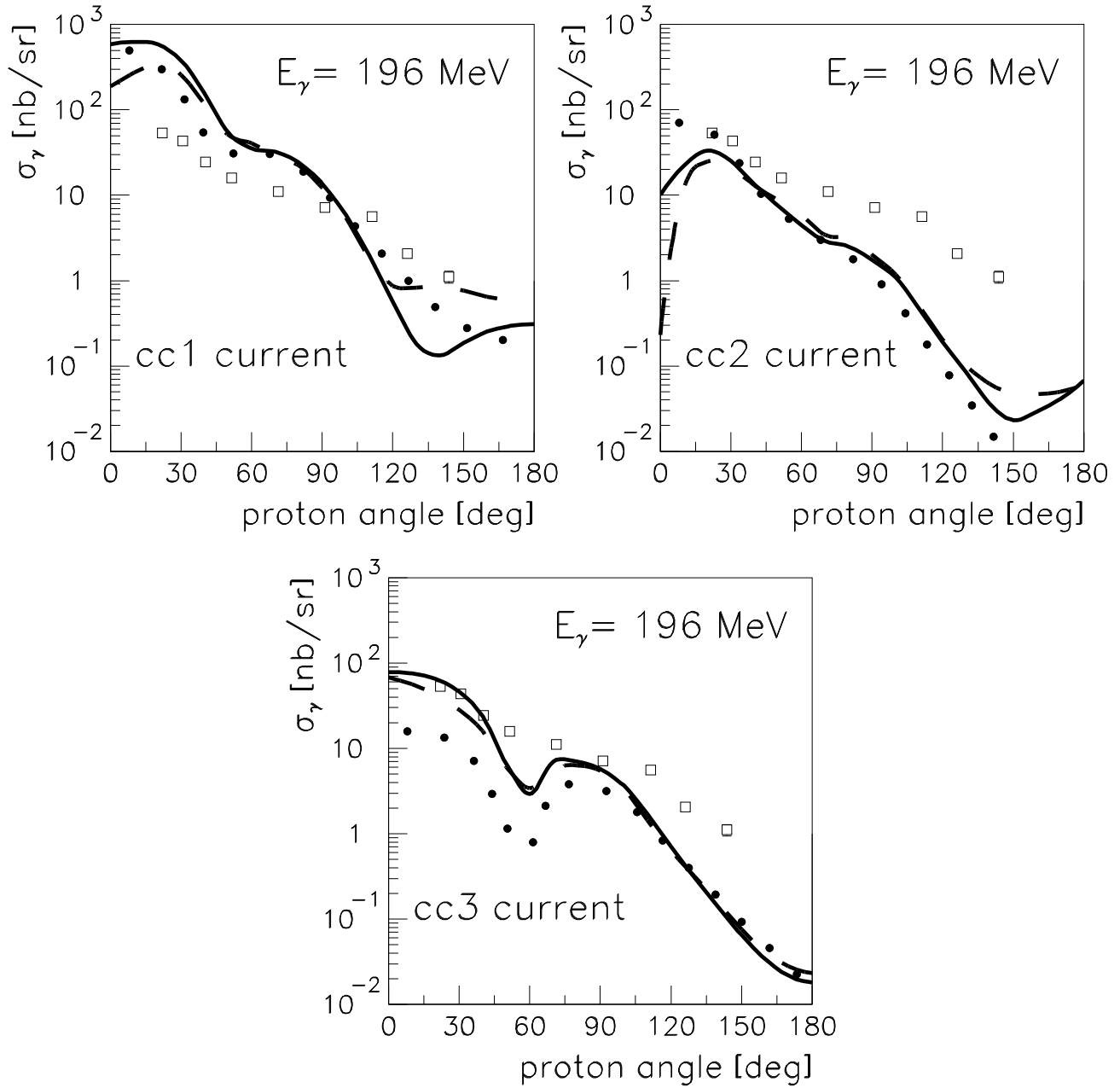


Figure 5: The same as in Fig. 4, but at $E_\gamma = 196$ MeV. The data are from Ref. [37].

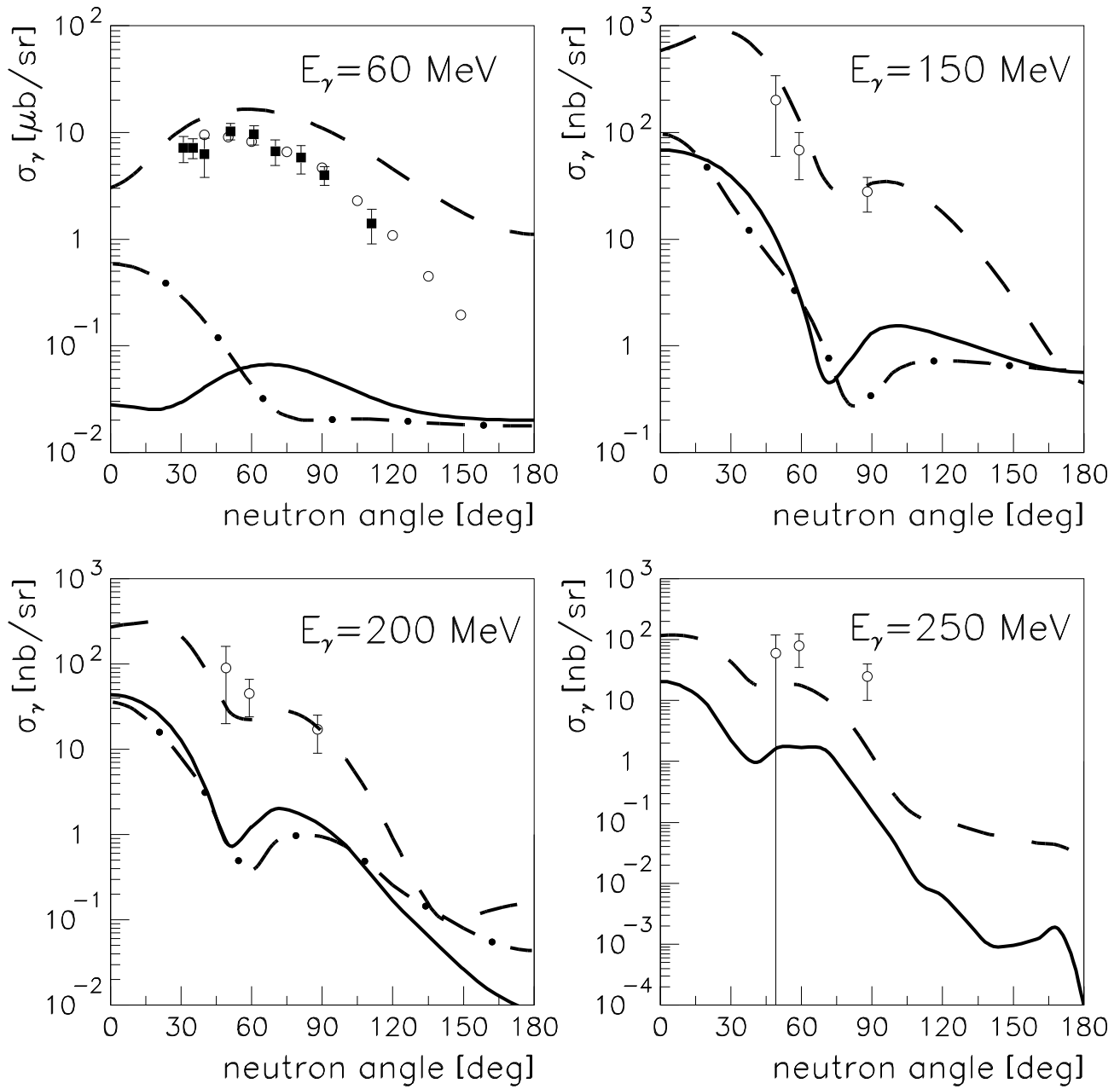


Figure 6: The cross section for the $^{16}\text{O}(\gamma, n)^{15}\text{O}_{\text{g.s.}}$ reaction as a function of the neutron scattering angle for photon energies ranging from 60 to 250 MeV. The data at 60 MeV are from Ref. [11] (black squares) and from Ref. [40] (open circles), and the data at 150, 200, and 250 MeV are from Ref. [41]. Line convention as in Fig. 1.